

RESEARCH ARTICLE

Voriconazole Compositated Polyvinyl Alcohol/Hydroxypropyl- β -Cyclodextrin Nanofibers for Ophthalmic Delivery

Xiaoyi Sun^{1‡a}, Zhenwei Yu^{2*}, Zhengyuan Cai¹, Lingyan Yu³, Yuanyuan Lv^{1*}

1 Department of Pharmacy, Zhejiang University City College, Hangzhou, Zhejiang, China, **2** Sir Run Run Shaw Hospital, College of Medicine, Zhejiang University, Hangzhou, Zhejiang, China, **3** Second Affiliated Hospital, School of Medicine, Zhejiang University, Hangzhou, Zhejiang, China

‡a Current address: Department of Pharmacy, Zhejiang University City College, Huzhou Street, Hangzhou, China

* zhenweiyu84@126.com (ZWY); lvyy@zucc.edu.cn (YYL)



OPEN ACCESS

Citation: Sun X, Yu Z, Cai Z, Yu L, Lv Y (2016) Voriconazole Compositated Polyvinyl Alcohol/Hydroxypropyl- β -Cyclodextrin Nanofibers for Ophthalmic Delivery. PLoS ONE 11(12): e0167961. doi:10.1371/journal.pone.0167961

Editor: Bing Xu, Brandeis University, UNITED STATES

Received: August 2, 2016

Accepted: November 23, 2016

Published: December 14, 2016

Copyright: © 2016 Sun et al. This is an open access article distributed under the terms of the [Creative Commons Attribution License](https://creativecommons.org/licenses/by/4.0/), which permits unrestricted use, distribution, and reproduction in any medium, provided the original author and source are credited.

Data Availability Statement: All relevant data are within the paper.

Funding: This work was supported by Public Welfare Technology Research and Social Development Project of Zhejiang (2013C33234: <http://www.zjkjt.gov.cn/> to ZWY), the National Nature Science Foundation of China (81402872 to XYs, 51303155 to YYL: <http://www.nsf.gov.cn/>), Natural Science Foundation of Zhejiang Province of China (LQ16H120004 to LYY and LY17H160002 to XYs: <http://www.zjnsf.gov.cn/>), and Health and Family Planning Commission of Zhejiang, China (2014RCA012 to ZWY: <http://www.zjwst.gov.cn/>).

Abstract

Voriconazole (VRC) incorporated in compositated polyvinyl alcohol (PVA)/hydroxypropyl- β -cyclodextrin (HP β CD) blended nanofibers were produced via electrospinning for efficient ophthalmic delivery. The VRC loading capacity increased with increasing HP β CD content. The optimal solution for electrospinning consisted of 8% (w/v) PVA, 4% (w/v) HP β CD and 0.5% (w/v) VRC. The nanofibers exhibited bead-free average fiber diameters of 307 \pm 31 nm and VRC was released *in vitro* in a sustained manner. The VRC nanofibers were characterized by infrared spectroscopy (FTIR), thermogravimetric analysis (TGA), differential scanning calorimetry (DSC) and scanning electron microscopy (SEM). The proton nuclear magnetic resonance (¹H-NMR) was used to analyze the molar ratio of HP β CD/VRC in the nanofibers. Compared with a VRC solution, the nanofibers significantly prolonged the half life, and increased the bioavailability of VRC in rabbit tears. No obvious signs of irritation were observed after application in the conjunctival sac. VRC nanofibers are promising for ophthalmic drug delivery and further pharmacodynamics studies are needed.

Introduction

Fungal keratitis, a fungal infection of the cornea, is one of the most serious ocular fungal infections. With the extensive application of broad-spectrum antibiotics and corticosteroids, the incidence of fungal keratitis has increased recently. It has become the major cause of blindness caused by ocular fungal infections [1, 2]. The first-line therapy for patients with fungal keratitis includes topical antifungal agents alone or in combination with systemic antifungal agents. However, the lack of specificity of antifungal agents is the main obstacle to successful therapy [3].

Voriconazole (VRC), a triazole antifungal agent, is a lipophilic drug (LogP 1.65) with low aqueous solubility (0.5 mg/ml in distilled water). It possesses promising characteristics such as broad-spectrum activity, activity against resistant fungal species, good oral bioavailability, and acceptable tolerability. It is highly effective against various fungal isolates associated with keratitis [4, 5]. It is commercially available as oral and i.v. preparations. However, adverse effects

The funders had no role in study design, data collection and analysis, decision to publish, or preparation of the manuscript.

Competing Interests: The authors have declared that no competing interests exist.

including visual disturbances, hepatic abnormalities and interactions with concomitant medications (attributed to its role as both an inhibitor and substrate of CYP2C19, CYP2C9, and CYP3A4) make topical application an attractive route of delivery [6, 7]. Topical VRC can penetrate the cornea, and therapeutic concentration can be achieved in the cornea, aqueous humor and vitreous body [8, 9]. To date, no topical formulation for ocular use has become commercially available, although several attempts involving cyclodextrin based eye drop solutions and gels [10, 11], microemulsions [12], liposomes [13], and niosomes [14] have revealed the potential of VRC for topical ophthalmic administration.

Electrospinning is a versatile and cost-effective method for producing nanoscale fibers from polymer solution or polymer melts with the help of a very strong electric field. Nanofibers have received great attention in tissue engineering, enzyme immobilization and drug delivery systems in recent years [15, 16]. The release [17, 18] and solubility [19] of poorly water-soluble drugs can be enhanced in nanofibers because of the large surface-to-volume ratios, highly nanoporous structures, short distances for diffusion and amorphous state of loaded drugs. If nanofibers are delivered to the cul-de-sac of the eye, they are easily wetted and swell. Effective drug concentrations in the eye can be achieved because of prolonged drug retention and controlled drug release from nanofibers [20]. To date, VRC-loaded nanofibers for oral use have been prepared. However, the polymer poly (ϵ -caprolactone) insolubility and long degradation time of such nanofibers makes them inappropriate for ocular applications [21]. There is a need to develop a hydrophilic system for VRC delivery. To the best of our knowledge, electrospun nanofibers for ophthalmic applications have not been previously investigated. In the present study, HP β CD was used in the formulation to solubilize VRC [11]. The application of cyclodextrins in ocular inserts has been reported previously [22]. Passive ocular permeation could be facilitated by increased drug concentrations at the ocular surface. Polyvinyl alcohol, a biocompatible polymer, has been widely used in ocular delivery systems [23]. The rational combination of PVA and cyclodextrin has previously been shown to be an efficient delivery technique [24]. Here, VRC and HP β CD have been incorporated in PVA nanofibers. The characteristics of the fibers and *in vitro* drug release, biocompatibility and pharmacokinetics in rabbit tears were investigated. The VRC nanofibers are safe for ocular use and they can significantly increase the half life and bioavailability of VRC in tears.

Materials and Methods

Materials

Polyvinyl alcohol (PVA AH-26) was supplied by Zhejiang Changqing Chemical Co., Ltd. VRC was purchased from Huahai Pharmaceutical Co, Ltd. (Taizhou, China). HP β CD from Fengyuan Biotechnology Co., Ltd (Jiangsu, China) and **cetonitrile** (Merck, Darmstadt, Germany) of HPLC grade were used. Male New Zealand white rabbits weighting 2.5–3.0 kg were purchased from Zhejiang Academy of Medical Science (Hangzhou, China). The rabbits were bred in normal way and all the animal experiments were performed in full compliance with guidelines approved by the Animal Care Committee at Zhejiang University City College. All efforts were made to minimize suffering.

Phase solubility studies

The solubility study was performed according to the method reported by Higuchi and Connors [25]. Excess VRC was mixed in an aqueous solution containing increasing amounts of HP β CD, which was agitated on a shaker at 37°C for 24 h. Then, the samples were centrifuged and the VRC contents were quantified using high-performance liquid chromatography (HPLC). The experiments were carried out in triplicate.

Preparation of VRC nanofibers

To determine the optimal concentration of PVA for the electrospinning process, 6%, 8% and 10% (w/v) PVA were used to prepare blank nanofibers. Subsequently, varied amounts of HP β CD were added to the polymer solution to achieve the final concentration of 4%, 6% and 8% (w/v). The effects of cyclodextrins on nanofibers morphology were determined. Finally, drug loaded spinning solutions were prepared by mixing PVA solutions with VRC dissolved in a HP β CD solution at 50°C. The finally solutions consisted of 8% (w/v) PVA, 4% (w/v) HP β CD and 0.5% (w/v) VRC (F1), 8% (w/v) PVA, 6% (w/v) HP β CD and 0.7% (w/v) VRC (F2), or 8% (w/v) PVA, 8% (w/v) HP β CD and 0.8% (w/v) VRC (F3).

The mixed solutions were then placed into a 20 mL plastic syringe equipped with a flat-tipped stainless steel needle ($d = 1.2$ mm). An emitting electrode of positive polarity from a high-voltage DC power supply (DW-P303-1ACFD, Dongwen High Voltage Supply, Tianjin, China) was connected to the spinning solution. A grounded copper plate was used as a collector. The electrostatic field strength was fixed at 18 kV/20 cm. The feed rate of the solution was controlled to 0.5 mL/h using a syringe pump (WZ-50C6, Smiths Medical Instrument Co., Ltd, Zhejiang, China). For the morphological study, the collection time was approximately 5 min, while, for the rest of the experiments, the collection time was 6 h. The collected nanofibers were placed in a vacuum oven overnight at 40°C to eliminate residual solvent.

Characterization of VRC nanofibers

Thickness. The thickness was measured with a hand-held micrometer (Mitutoyo, Japan). The values were determined at five different regions of the film.

Scanning electron microscope (SEM). The morphological appearance of the nanofibers was assessed using a scanning electron microscope (SEM, TM-1000, Hitachi, Japan). The average diameter of the fibers was evaluated using Image J software by measuring 100 fibers from the SEM images.

The proton nuclear magnetic resonance ($^1\text{H-NMR}$) analysis. The proton nuclear magnetic resonance ($^1\text{H-NMR}$) spectra were recorded at 400 MHz (Bruker, AVANCE III 400, Switzerland). 5 mg VRC, 10 mg PVA/HP β CD nanofibers or 10 mg VRC nanofibers were dissolved in 0.5 mL d_6 -DMSO.

Thermogravimetric analysis (TGA). Thermogravimetric (TGA, TA Q50, USA) analyses were performed for VRC, HP β CD, PVA, PVA/HP β CD nanofibers and VRC nanofibers. TGA was conducted under nitrogen atmosphere by heating the samples from 50 to 600°C at the heating rate of 20°C/min.

Differential scanning calorimetry (DSC). A differential scanning calorimeter (DSC, Q20, TA, USA) was used to investigate the thermal behavior of the VRC nanofibers. The DSC thermograms (equilibrated with an indium standard; each sample weighed 3–5 mg) were obtained during heating from 35 to 260°C at a rate of 10°C/min.

Fourier transform infrared spectrophotometry (FT-IR). The chemical structures of VRC nanofibers and PVA/HP β CD nanofibers were characterized using a Fourier transform infrared spectrophotometry (FT-IR, Nicolet 6700, USA) with the accessories of attenuated total reflectance (ATR). VRC were ground and pressed into KBr dishes pellets before analysis from 400 to 4,000 cm^{-1} .

In vitro release

Nanofiber films containing 3 mg of VRC were immersed in 100 mL of 0.9% NaCl at 32°C with shaking at 50 rpm. The release medium was sampled (1 mL) for the drug assay and an equal

amount of fresh medium was added at the times indicated. Before the HPLC assay, the samples were diluted with [acetonitrile](#). A VRC solution was used as a control.

Pharmacokinetics in rabbit tears

Eight rabbits were separated into a nanofiber-treated group and a VRC solution-treated group. VRC solution was prepared by dissolving VRC in a 0.9% (w/v) HPβCD solution to achieve a final 0.15% (w/v) drug concentration.

Rabbits were treated with a single administration of 40 μL of VRC solution or 1.5 mg of nanofibers, in which the drug dose was equivalent to that of the VRC solution. Tear fluid samples were collected at 0.25, 0.5, 0.75, 1.0, 2.0, 3.0, 4.0, 6.0, 8.0, 12.0, and 24.0 h after administration in the nanofiber group and at 0.25, 0.5, 0.75, 1.0, 2.0, 3.0, 4.0, 6.0, and 8.0 h after administration in the VRC solution group, using filter papers, which were weighed before use and gently inserted into the inferolateral cul-de-sac of the eye, close to the middle of the eye, for 30 seconds. After collection, papers were weighed again. Then, the papers were dried under stream of nitrogen gas and vortexed with 500 μL of methanol for 5 min. After centrifugation (12,000 rpm) for 10 min, the organic phase was transferred to another tube and evaporated to dryness. The residue was reconstituted with 50 μL methanol. The drug concentration in each sample was determined using HPLC.

Ocular irritation test

An ocular irritation test (Draize eye test) was used to evaluate the ocular tolerance of the nanofibers.

Eight rabbits were randomly divided into two groups. One eye of the rabbit was treated with the VRC solution or VRC nanofibers, while the untreated eye functioned as a control. A successive administration once a day for 7 days was performed at the same dosages as those used in the pharmacokinetic study. The ocular irritation was observed at 1, 8 and 24 h after administration. The animals' discomfort and symptoms in the conjunctiva, cornea, and lids were macroscopically examined using the Acute Eye Irritation/Corrosion scoring system established by the 2012 Organization for Economic Cooperation and Development for ocular irritation testing ([Table 1](#)) [26].

At the end of the test, the rabbits were euthanized by injection of a lethal dose of pentobarbital into the marginal ear vein. The cornea tissues were collected and fixed by immersion in buffered formalin (pH 7.4), dehydrated and embedded in paraffin. Sections were stained with hematoxylin and eosin (H&E) to evaluate potential injury to the cornea.

HPLC analysis of VRC

The drug content in the VRC nanofibers was quantified by dissolving them in 30% (v/v) ethanol. The solutions were analyzed using HPLC. Drug loading rate (DL) was calculated:

$$DL(\%) = \frac{M_{VRC}}{M_{NF}} \times 100\%$$

Table 1. Grading of ocular irritation test.

Grade	Cornea	Conjunctiva	Discharge	Lids
0	No alternations	No alternations	No discharge	No swelling
1	Mild opacity	Mild hyperemia; mild edema	Mild discharge without moistened hair	Mild swelling
2	Intense opacity	Intense hyperemia; Intense edema; Hemorrhage	Intense discharge with moistened hair	Obvious swelling

doi:10.1371/journal.pone.0167961.t001

where M_{VRC} is the actual VRC content in the weighed quantity of nanofibers, and M_{NF} is the weighed quantity of nanofibers.

The HPLC system used was of the Agilent 1260 series (Agilent, USA) and detection conditions were as follows: Agilent ZORBAX SB-C₁₈ column(250 mm × 4.60 mm, 5 μm); flow rate: 1.0 mL/min; the UV detector wavelength: 256 nm. The mobile phase was acetonitrile: water (46:54).

Statistical analysis

Kinetic[™] V.4.4 with a non-compartment model was utilized to calculate the pharmacokinetics parameters in rabbit tears. Statistical data were analyzed using a Student's t-test and a *P*-value of 0.05 was considered to be significant.

Results and Discussion

VRC dissolved in HPβCD solution

HPβCD, a cyclic oligosaccharide with an outer hydrophilic surface and a lipophilic cavity, is the most thoroughly studied cyclodextrin derivative. Numerous toxicological studies, pharmaceutical technological experiments and human clinical trials have been performed with HPβCD [27]. It is capable of forming inclusion complexes with VRC [28]. To increase the drug content in the nanofibers, we added HPβCD to the electrospinning solution. [Fig 1](#)

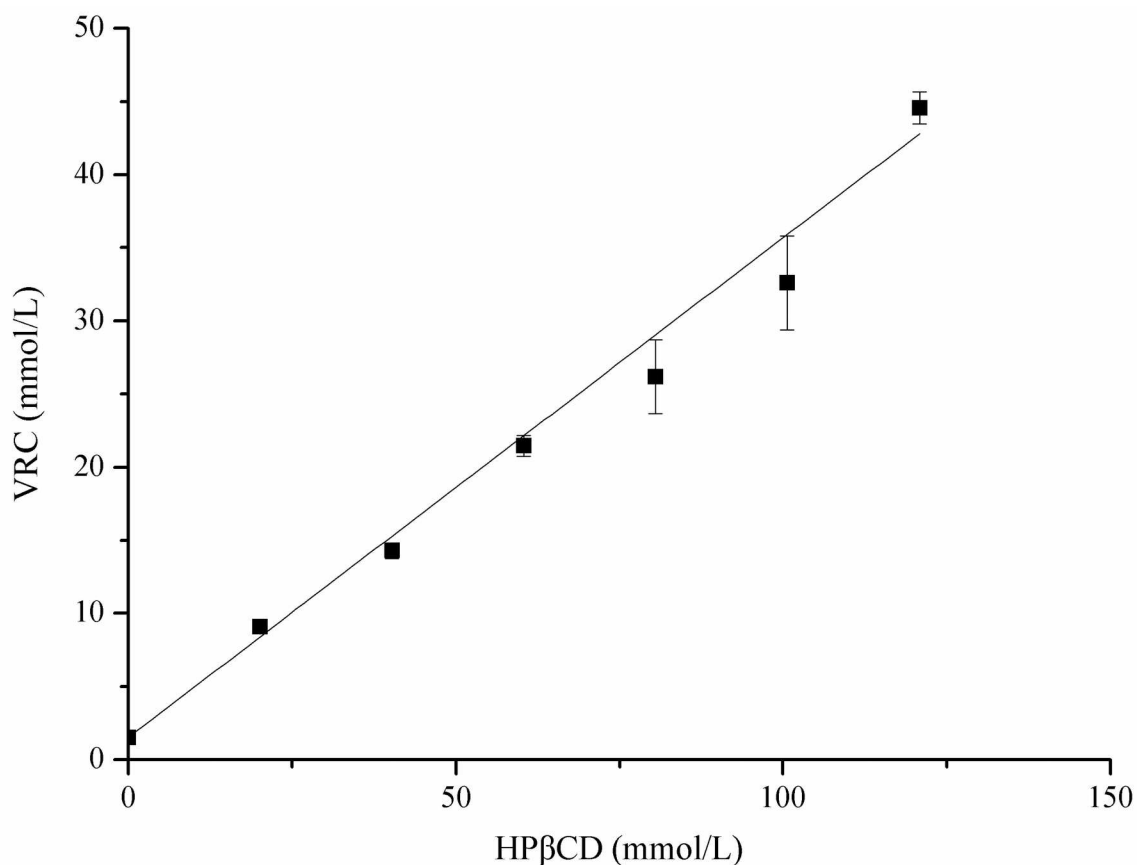


Fig 1. Solubility diagram for VRC in HPβCD at 37°C.

doi:10.1371/journal.pone.0167961.g001

displays a linear increase in the solubility of VRC as a function of HP β CD concentration at 37°C, which displays a typical A_L type, according to Higuchi and Connors, indicating the formation of soluble complexes of a 1:1 stoichiometry [25]. The apparent stability constant (K_c) value was estimated to be 320 L/mol, according to the following equation [29]:

$$K_c = \frac{slop}{C_0 \times (1 - slop)}$$

where the slop was calculated by [linear regression](#) of the profile and C_0 was the solubility of VRC in H₂O. Compared with [sulfobutylether- \$\beta\$ -cyclodextrin](#) (SBE- β -CD) used in VRC injections [30], HP β CD bears no ionizable groups, which results in a low conductivity, facilitating the preparation of nanofibers. Moreover, the solubilization capacity of HP β CD is comparable with that of SBE- β -CD.

Fabrication of VRC-loaded nanofibers

To prepare the nanofibers, the PVA concentration was first optimized. The blank nanofibers were fabricated using PVA with varied concentrations ([Fig 2A1-A3](#)). Bead-free and smooth fibers could be prepared using PVA solutions below 8% (w/v). The diameters were 204±23 nm, 210±31 nm, and 554±175 nm for fibers electrospun using 6%, 8% and 10% (w/v) PVA solutions, respectively. When the PVA concentration increased to 10%, fiber aggregations and fibers heterogeneity were observed and mean fiber diameters significantly increased. This was attributed to the increase in the viscosity of the spinning solution. The electrostatic field force was not enough to stretch the polymer to a uniform structure. Considering its higher spinning efficiency, we chose an 8% PVA solution for further investigation. Subsequently, varied amounts of HP β CD were added. Incorporation of HP β CD in the nanofibers did not alter the fiber [morphology](#) ([Fig 2B1-B3](#)). Inclusion of 4%, 6% and 8% (w/v) HP β CD in the spinning solution resulted in fiber diameters of 197±32nm, 212±32 nm, and 202±26 nm, respectively.

HP β CD could increase the solubility of VRC, and the enhancement was dependent on HP β CD concentration ([Fig 1](#)). To increase the drug content in the nanofibers, different amounts of HP β CD in conjunction with different levels of VRC were added to the spinning solution. Increasing the amounts of HP β CD and VRC resulted in an increase in the diameter of the drug loaded nanofibers. Similar results have also been reported for herbal oil loaded nanofibers [31]. The diameter of the nanofibers (F1) was 307±31 nm ([Fig 2C1](#)). When the HP β CD concentration was changed to 6%, the VRC content increased to 0.7% (F2), and the resultant nanofiber size was 315±123 nm ([Fig 2C2](#)). A higher concentration of VRC (0.8%) with 8% HP β CD (F3), resulted in the formation of beaded fibers ([Fig 2C3](#)). The actual drug loading rates of F1, F2 and F3 were 3.7±0.05%, 4.6±0.01% and 4.5±0.01%, respectively, which are much higher than those of nanofibers without HP β CD (below 1%), which were measured in a preliminary study. The addition of HP β CD rendered the nanofibers suitable for clinical application. The obtained nanofibers were used in an *in vitro* release study.

The dissolution profiles in [Fig 3](#) show a significant delayed VRC release from the nanofibers compared with the VRC powder. More than 90% of the VRC powder was dissolved within 0.5 h. However, complete drug release was achieved after 2 h in the three nanofiber groups. Slower release from nanofibers with a higher PVA/HP β CD ratio was observed. The F1 fibers with a PVA/HP β CD ratio of 2:1 showed the slowest release among the nanofiber samples. VRC demonstrated sustained release from the nanofibers for 6 h. PVA is a linear, synthetic polymer traditionally used in pharmaceutical science because of its superior mechanical properties and high biocompatibility. This polymer can be included in tablets [32], microparticles [33], hydrogels [34], and patches [35] that swell and release entrapped drugs in a sustained way. The

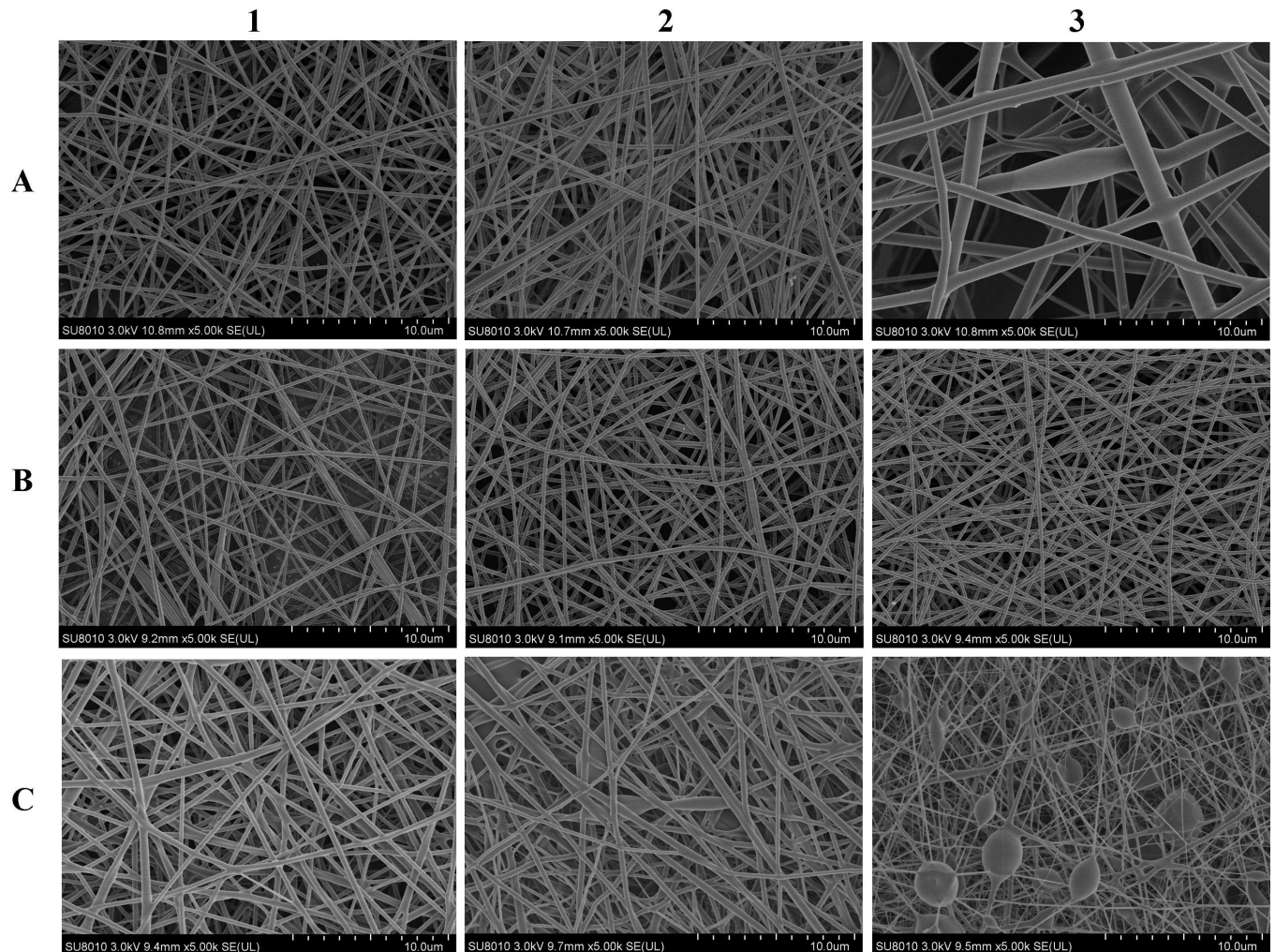


Fig 2. SEM images (x5000) of nanofibers fabricated by spinning solutions containing A1 6% PVA. A2 8% PVA. A3 10% PVA. B1 4% HPβCD, 8% PVA. B2 6% HPβCD, 8% PVA. B3 8% HPβCD, 8% PVA. C1 0.5% VRC, 4% HPβCD, 8% PVA (F1). C2 0.7% VRC, 6% HPβCD, 8% PVA (F2). C3 0.8% VRC, 8% HPβCD, 8% PVA (F3).

doi:10.1371/journal.pone.0167961.g002

drug release rates are governed by the drug diffusion and polymer dissolution (surface erosion) [36]. Drug solubility, polymer molecular weight, polymer concentration and excipients are factors that affect the release profiles. In the present study, soluble HPβCD/VRC complex can readily diffuse from hydrogel matrix when the polymer concentration is relatively low. Inadequate PVA in F2 and F3 where the PVA/HPβCD mass ratios were 1.33:1 and 1:1 resulted in a faster release from the polymer matrix. All the fibers exhibited an initial burst release as a result of the immediate dissolution of the drug which became associated with the fiber surface during the electrospinning process [18]. F1 was chosen as the optimal formulation for *in vivo* evaluation, because of its defect free morphology, slow release, and relatively high drug loading.

Characterization of the F1 VRC nanofibers

Cylindrically shaped continuous nanofibers without non-connected ‘tailed’ beads were formed (Fig 2C1). The average diameter of these fibers was approximately 300 nm. No drug crystals or other kinds of drug aggregates were observed on the surface of the fibers. It was presumed that

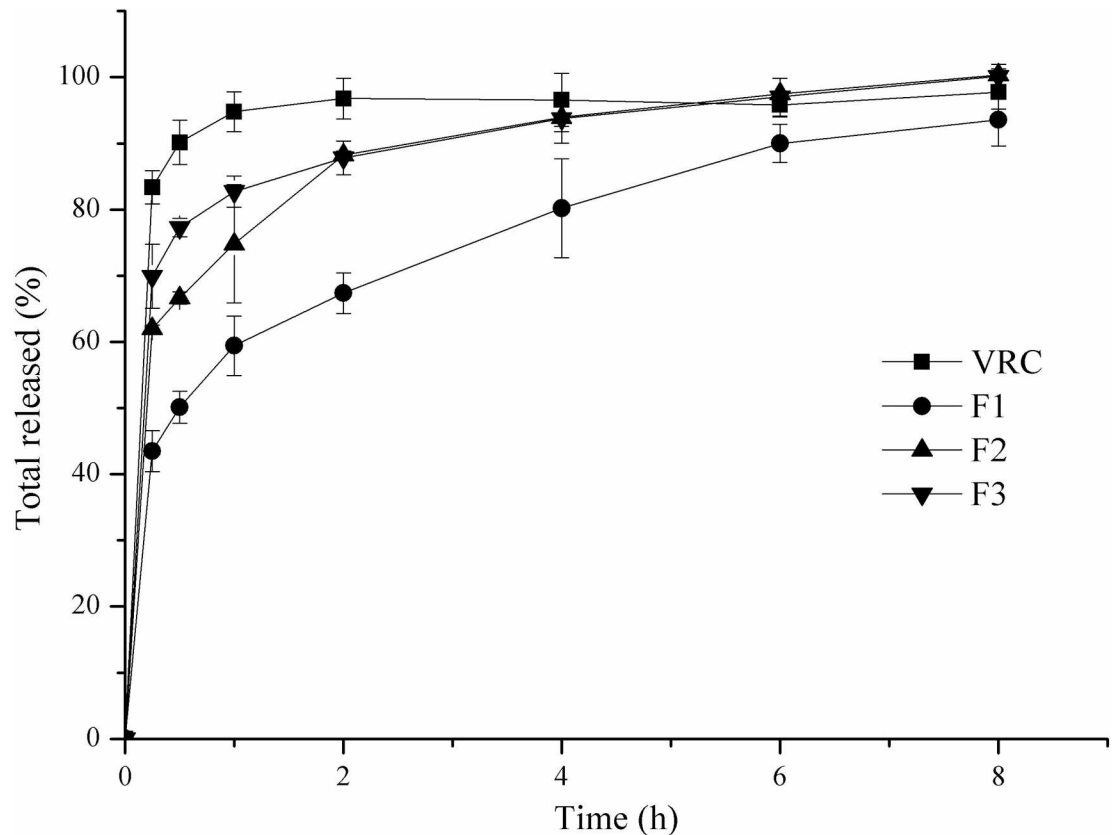


Fig 3. In vitro release of VRC electrospun nanofibers.

doi:10.1371/journal.pone.0167961.g003

the VRC was homogeneously distributed in the spinning fibers owing to the increased solubility of the inclusion complex and interactions between PVA and VRC. The average thickness of the electrospun film was $235.6 \pm 11.2 \mu\text{m}$. Taking into account the thickness of Ocuser[®] ($300 \mu\text{m}$), few tolerance problems should be expected after application in the conjunctival sac [37].

Proton nuclear magnetic resonance ($^1\text{H-NMR}$) was employed to further explore the molar ratio of HP β CD/VRC in nanofibers (Fig 4). The characteristic peaks of VRC $^1\text{H-NMR}$ (d₆-DMSO), δ (ppm): 9.05 (d, 1H), 8.24 (s, 1H), 8.08 (d, 1H), 7.63 (s, 1H), 6.95–6.91 (m, 3H), 2.51–2.5 (m, 2H), 1.11 (d, 3H) and HP β CD: 1.03 (s, 21H) were showed in the spectra of VRC nanofibers. The results indicated that VRC as well as HP β CD were electrospun in the nanofibers. In order to make the molar ratio calculations, the integration of HP β CD and VRC peaks were used. The molar ratio of HP β CD: VRC in nanofibers was calculated as 1:0.54 by taking the integration of the protons of HP β CD at 1.03 ppm and VRC at 1.11 ppm. According to the actual drug loading rate determined by HPLC, the molar ratio was calculated as 1:0.5. $^1\text{H-NMR}$ results was in good consistence with HPLC results. Substantial amount of VRC was incorporated in nanofibers during the preparation and electrospinning.

TGA thermograms of VRC, HP β CD, PVA, PVA/HP β CD nanofibers and VRC nanofibers are given in Fig 5. The initial weight loss below 100°C was due to water loss. In the TGA curves of VRC and HP β CD, the major weight loss above 172.41°C and 320.69°C corresponded to the main thermal degradation of VRC and HP β CD. PVA powders exhibited three-step degradation: a small mass loss started below 185.17°C , a large loss took place in the temperature range

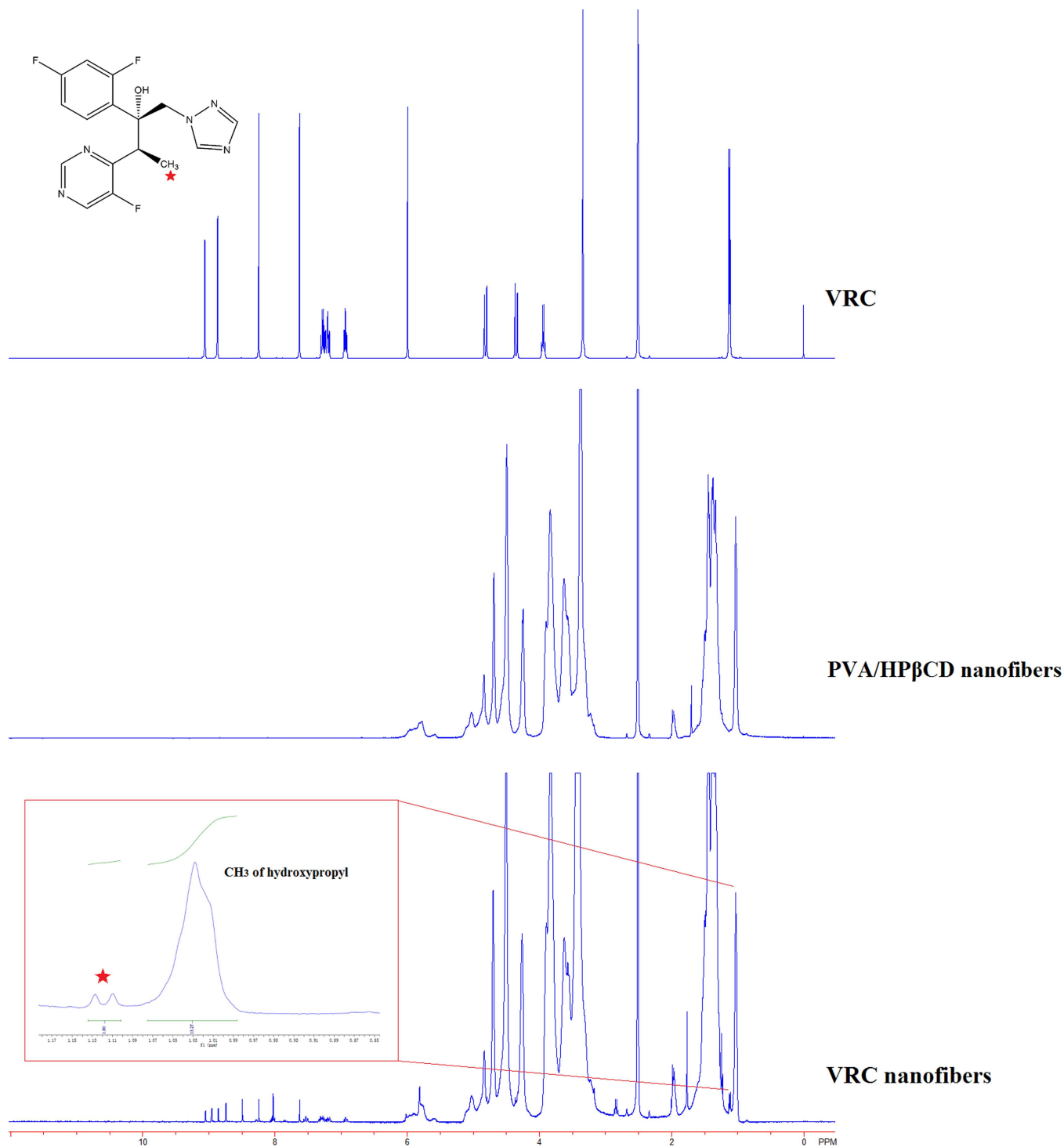


Fig 4. ¹H-NMR spectra of VRC, PVA/HPβCD nanofibers and VRC nanofibers. The insert was the integration of VRC peak (1.11 ppm) and HPβCD peak (1.03 ppm).

doi:10.1371/journal.pone.0167961.g004

of 258.28–408.96°C, and a medium mass loss took place in the range of 409–518.97°C. In the case of PVA/HPβCD nanofibers, the three decomposition stages of PVA and thermal degradation behavior of HPβCD were observed. The second weight loss in VRC nanofibers were

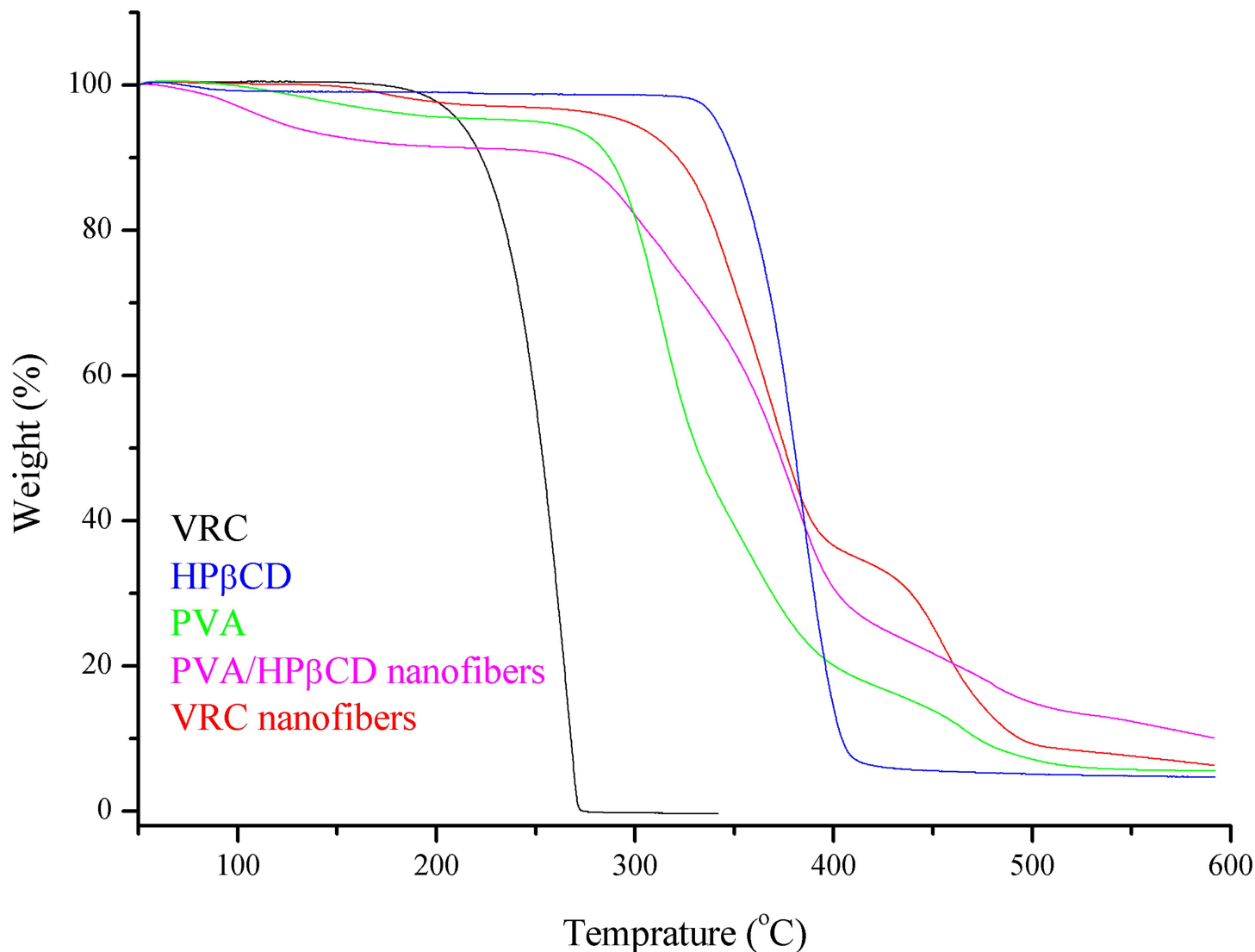


Fig 5. TGA thermograms of VRC, HPβCD, PVA, PVA/HPβCD nanofibers and VRC nanofibers.

doi:10.1371/journal.pone.0167961.g005

between 274.48 to 400.69°C. The shifting of thermal degradation onset of VRC from 172.41°C to higher temperature suggested the existence of inclusion complex between HPβCD and VRC. Thermal stability of VRC was elevated in VRC nanofibers.

DSC studies were undertaken to evaluate the physical state of VRC in the electrospun nanofibers and the thermograms are shown in Fig 6. Both HPβCD and PVA powders exhibited broad endothermic peaks between 60 and 160°C, and these peaks correspond to the dehydration of HPβCD and PVA. The melting temperatures (T_m) for PVA was 218.42°C obtained from the DSC scan of PVA powders. Two endothermic peaks at around 120 and 215°C corresponding to the characteristic peaks of HPβCD and PVA were observed in PVA/HPβCD nanofibers. The thermogram of the VRC powder exhibited a melting point at 132.44°C whereas no melting point was observed for the VRC nanofibers, suggesting that VRC was incorporated into nanofibers in an amorphous state.

The FT-IR spectra of the VRC powder, PVA powder, HPβCD powder, PVA/HPβCD nanofiber and VRC nanofiber are displayed in Fig 7. The spectra of the PVA and HPβCD powders

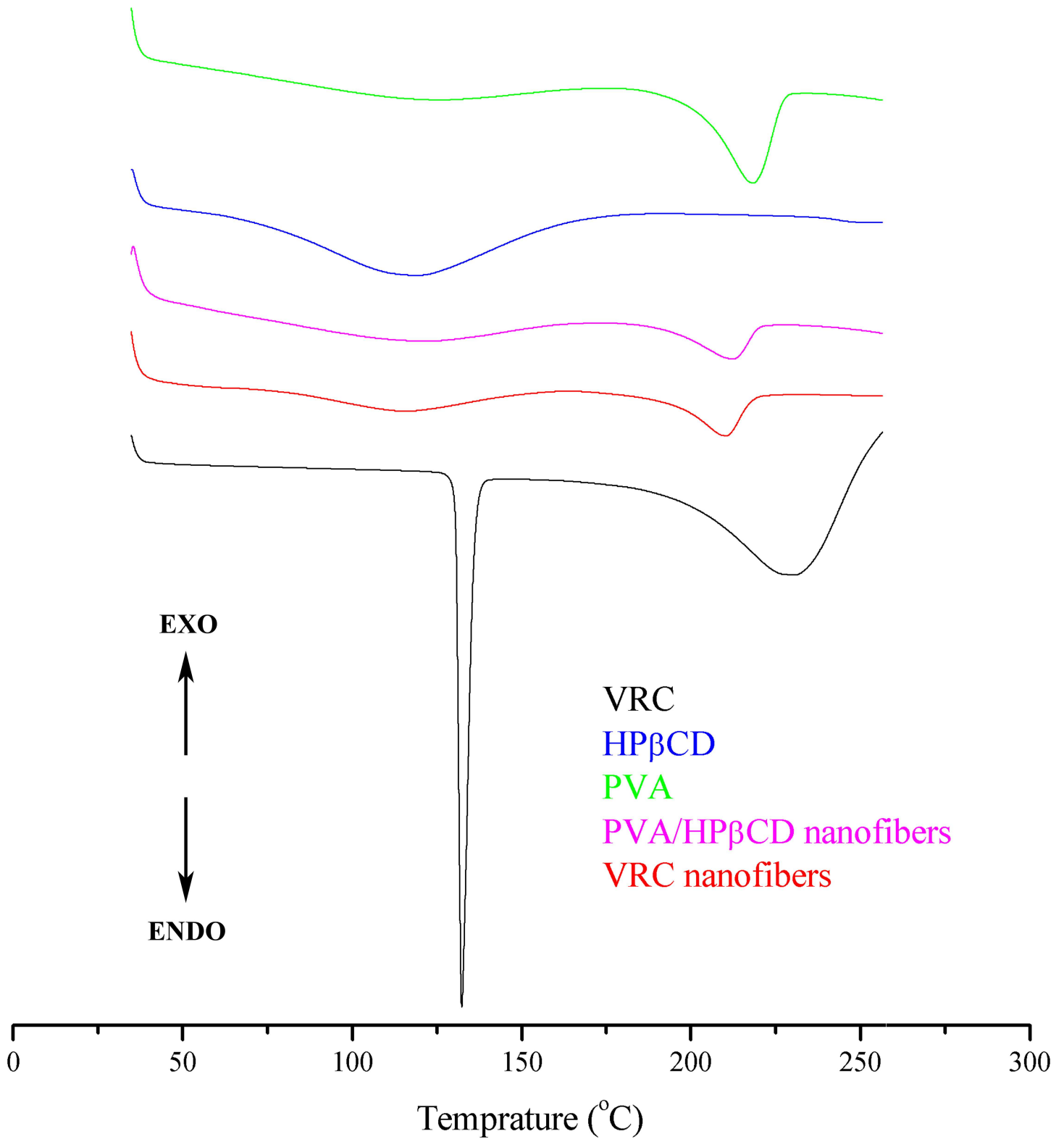


Fig 6. DSC thermograms of HPβCD, PVA, VRC, PVA/HPβCD nanofibers and VRC nanofibers.

doi:10.1371/journal.pone.0167961.g006

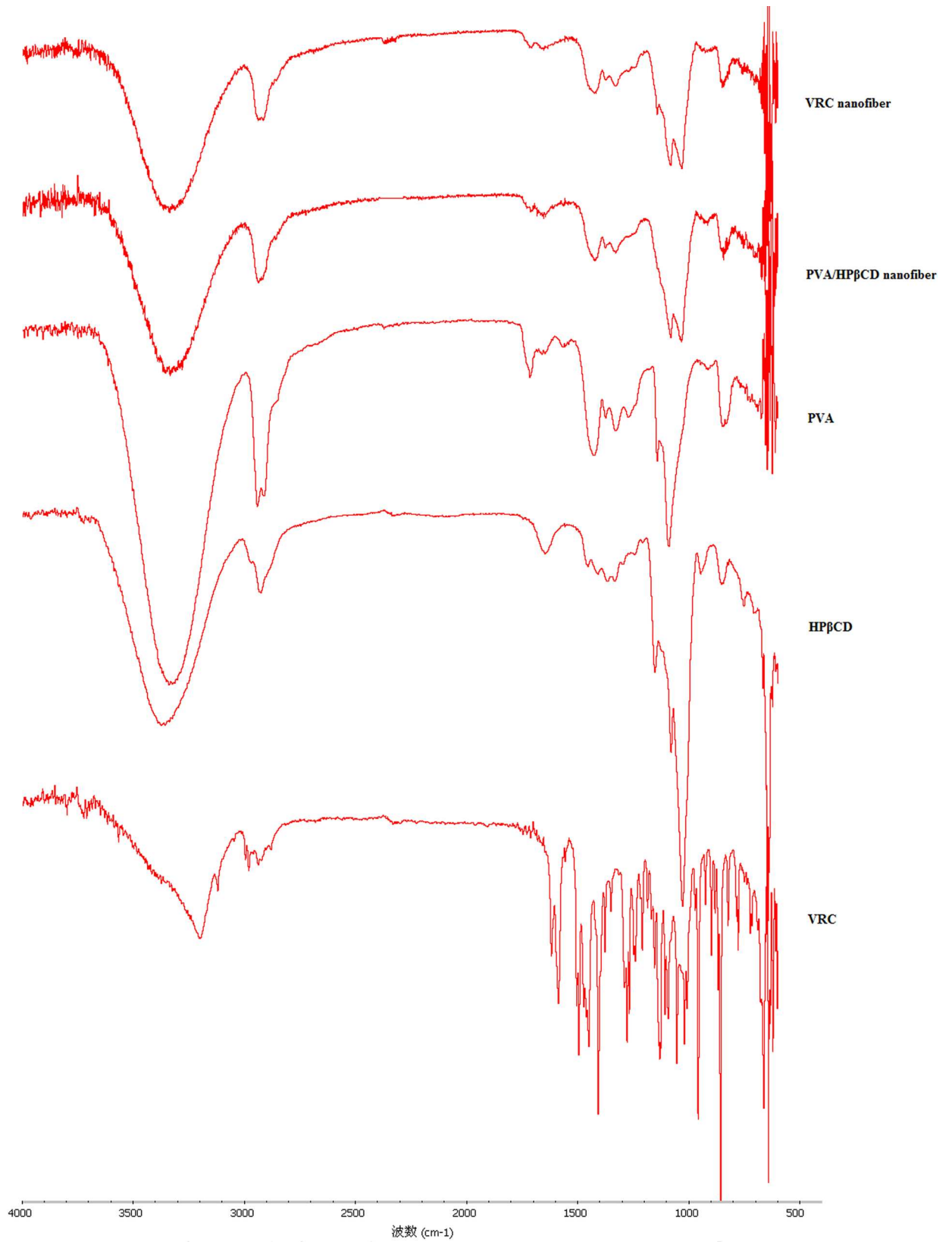


Fig 7. FT-IR spectra of VRC, PVA, HPβCD, PVA/HPβCD nanofibers and VRC electrospun nanofibers.

doi:10.1371/journal.pone.0167961.g007

exhibited absorption peaks around 3350, 2930, and 1090 cm^{-1} that are attributed to the stretching vibrations of OH, CH and CO, respectively [38]. The VRC powder exhibited absorption peaks at 3200 cm^{-1} corresponding to the stretching vibrations of OH. The bands at 3000–2850, 1600–1400, and 1360–1250 cm^{-1} were assigned to the alkane CH, C = C aromatic and aryl C-N stretches [39]. The dominant absorption peaks observed in PVA and HP β CD were also observed in spectra of PVA/HP β CD nanofibers. VRC nanofibers displayed only the typical bands of PVA/HP β CD nanofibers, indicating that free VRC cannot be detected in the sample. This might actually indicate that VRC was completely included in the cyclodextrin cavity, as observed in VRC-cyclodextrin complexes [39]. There were interactions between VRC and HP β CD. The similar results were also obtained in itraconazole-cyclodextrin complex. The disappearance of FTIR bands was considered to be credible evidence for the presence of inclusion complexes [40, 41]. During our preparing of spinning solution, there was no purification process, and therefore there should be free VRC in the nanofibers [38]. However, VRC solubility in water is low. The insoluble VRC in the nanofibers is negligible. Therefore, the free VRC characteristic peak was not visible in the FT-IR spectra.

Pharmacokinetics in rabbit tears

The majority of ophthalmic treatments are delivered as highly concentrated eye drops. They suffer from short precorneal residence time which is associated with low corneal drug absorption. Nasolachrymal drainage, lacrimal replacement and the relative impermeability of the corneal epithelial membrane lead to rapid and extensive loss of drugs from the precorneal area [42]. Therefore, in this study we developed nanofibers which formed three-dimensional networks with the ability to swell in aqueous solvents in a controlled manner [18], with the aim to achieve higher bioavailability and controlled ocular delivery. As an effective antifungal concentration [11, 12], we set the dose at 60 μg for the pharmacokinetics study. The established HPLC method for VRC determination met the *in vivo* analytical requirements. The low limit of quantification and low limit of detection of the method were 0.1 $\mu\text{g}/\text{mL}$ and 0.03 $\mu\text{g}/\text{mL}$, respectively. The extraction recoveries at low, medium and high VRC levels were all greater than 90%. The standard curve for the drug assay in rabbit tears was $Y = 418921X - 21369$ within 0.1–10 $\mu\text{g}/\text{mL}$ VRC. The standard curve showed good linearity and the R^2 was 0.9991.

The drug tear concentration-time profiles of the two formulations are shown in Fig 8. The VRC solution group achieved a higher drug concentration in the first 15 min, but it was eliminated rapidly. The drug was undetectable at 4 h. However, in the nanofiber group, the drug tear concentrations were all above 0.5 $\mu\text{g}/\text{mL}$ until 24 h. The data were in accordance with the sustained drug release profiles of nanofibers *in vitro*. The calculated pharmacokinetic parameters are listed in Table 2, and the differences were mathematically evaluated by the calculation of $t_{1/2}$ and AUC_{0-t} . The nanofibers significantly prolonged the VRC half-life in tears, and increased the VRC bioavailability. Compared with the VRC solution, the relative bioavailability was 245%. The interaction of HP β CD with biological membranes has been reported to facilitate drug absorption in the tear film [43]. In addition to the prolonged residence time, a higher ocular drug bioavailability was achieved in the current study. Therefore, these nanofibers are expected to be effective in treating against fungal keratitis.

Ocular irritation test

PVA, which formed the nanofiber matrix, is a well-tolerated polymer type for ophthalmic drug delivery systems [24, 44]. HP β CD has also previously been shown to be safe in aqueous eye drop solutions, even at high concentrations [45]. In addition, the moderate thickness of the ocular nanofiber film means that it is unlikely to cause irritation.

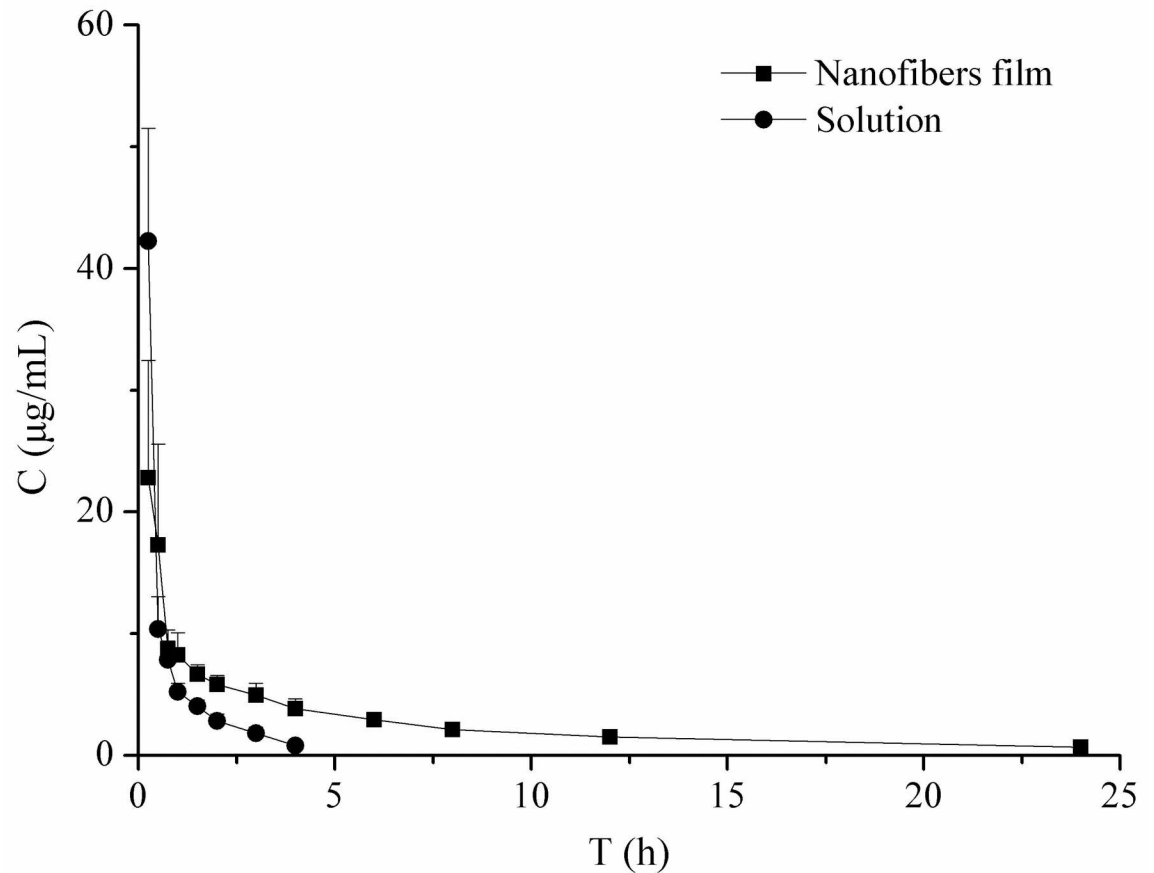


Fig 8. Concentration-time curves of VRC in tears after topical application of VRC solution or VRC-loaded nanofibers to the rabbit eye (n = 4, $\bar{x} \pm SD$).

doi:10.1371/journal.pone.0167961.g008

The Draize eye test results show that there was no ocular discomfort after the administration of the VRC nanofibers and the VRC solution (Fig 9A–9C). According to the Draize scoring standard, the eye irritation reaction scores were 0 for both groups. The H&E micrographs of the corneas (Fig 9D–9F) exhibit intact corneal structures and epithelia without histopathological abnormalities in the animals treated using the nanofibers. The results suggested that the VRC composited PVA/HP β CD nanofibers are a promising non-irritant system.

Conclusion

In this research work, we successfully developed VRC incorporated PVA/HP β CD nanofibers for the treatment of fungal keratitis. The physicochemical characteristics, pharmacokinetics and ocular irritation of the optimized fibers were evaluated. SEM, TGA, DSC and FT-IR

Table 2. Pharmacokinetic parameters of VRC in rabbit tears ($\bar{x} \pm SD$, n = 4).

	$AUC_{0 \rightarrow \infty} (\mu\text{g} \cdot \text{h} \cdot \text{mL}^{-1})$	$t_{1/2} (\text{h})$
Solution	26.56 \pm 1.87	1.24 \pm 0.35
Nanofibers	64.69 \pm 10.51*	8.47 \pm 2.59*

* Compared with that of the solution group, $P < 0.05$

doi:10.1371/journal.pone.0167961.t002

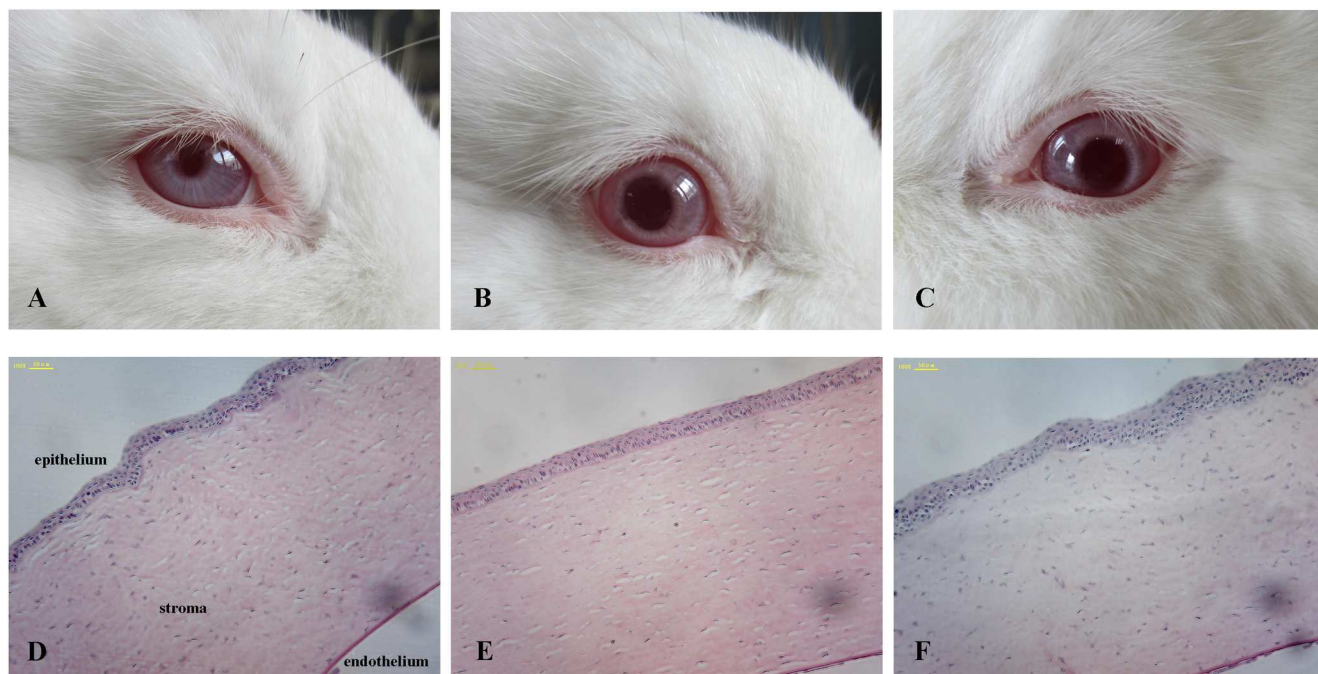


Fig 9. Results of irritation test at day 7 after the administration of VRC nanofibers or VRC solution. A-C Images of rabbit eyes. D-F Optical micrographs of corneal tissue (A, D Control. B, E VRC solution. C, F VRC nanofibers).

doi:10.1371/journal.pone.0167961.g009

analyses suggest that VRC is present in an amorphous state in the nanofibers and there are interactions between VRC and HP β CD. Drug loading was increased because of the solubilization effect of HP β CD. A sustained release of VRC for 24 h was achieved. The half-life, $AUC_{0 \rightarrow 24}$ and bioavailability of VRC were all significantly increased in rabbit tears. Furthermore, few tolerance problems were observed after consecutive application for 7 days. It can be concluded that these nanofibers represent a promising delivery system to prolong the ocular delivery of VRC.

Author Contributions

Conceptualization: XYS ZWY YYL.

Data curation: XYS ZYC ZWY.

Formal analysis: ZWY LYY.

Funding acquisition: XYS ZWY LYY YYL.

Investigation: XYS ZYC ZWY LYY YYL.

Methodology: XYS ZWY YYL.

Project administration: XYS ZWY.

Resources: XYS ZWY YYL.

Software: XYS.

Supervision: ZWY YYL.

Validation: XYS ZYC ZWY.

Visualization: XYS.

Writing – original draft: XYS LYY.

Writing – review & editing: ZWY YYL.

References

1. Iyer SA, Tuli SS, Wagoner RC. Fungal keratitis: emerging trends and treatment outcomes. *Eye Contact Lens*. 2006; 32:267–271. doi: [10.1097/01.icl.0000249595.27520.2e](https://doi.org/10.1097/01.icl.0000249595.27520.2e) PMID: [17099386](https://pubmed.ncbi.nlm.nih.gov/17099386/)
2. Gower EW, Keay LJ, Oechsler RA, Iovieno A, Alfonso EC, Jones DB, et al. Trends in fungal keratitis in the United States, 2001 to 2007. *Ophthalmology*. 2010; 117:2263–2267. doi: [10.1016/j.ophtha.2010.03.048](https://doi.org/10.1016/j.ophtha.2010.03.048) PMID: [20591493](https://pubmed.ncbi.nlm.nih.gov/20591493/)
3. Shivaprakash MR, Geertsens E, Chakrabarti A, Mouton JW, Meis JF. In vitro susceptibility of 188 clinical and environmental isolates of *Aspergillus flavus* for the new triazole isavuconazole and seven other antifungal drugs. *Mycoses*. 2011; 54:e583–e589. doi: [10.1111/j.1439-0507.2010.01996.x](https://doi.org/10.1111/j.1439-0507.2010.01996.x) PMID: [21518026](https://pubmed.ncbi.nlm.nih.gov/21518026/)
4. DiDomenico B. Novel antifungal drugs. *Curr Opin Microbiol*. 1999; 2:509–515. PMID: [10508731](https://pubmed.ncbi.nlm.nih.gov/10508731/)
5. Lat A, Thompson GR. Update on the optimal use of voriconazole for invasive fungal infections. *Infect Drug Resist*. 2011; 4:43–53. doi: [10.2147/IDR.S12714](https://doi.org/10.2147/IDR.S12714) PMID: [21694908](https://pubmed.ncbi.nlm.nih.gov/21694908/)
6. Jeong S, Nguyen P D, Desta Z. Comprehensive in vitro analysis of voriconazole inhibition of eight cytochrome P450 (CYP) enzymes: major effect on CYPs 2B6, 2C9, 2C19, and 3A. *Antimicrob Agents Chemother*. 2009; 53:541–551. doi: [10.1128/AAC.01123-08](https://doi.org/10.1128/AAC.01123-08) PMID: [19029318](https://pubmed.ncbi.nlm.nih.gov/19029318/)
7. Nivoix Y, Levêque D, Herbrecht R, Koffel JC, Beretz L, Ubeaud-Sequier G. The enzymatic basis of drug-drug interactions with systemic triazole antifungals. *Clin Pharmacokinet*. 2008; 47:779–792. doi: [10.2165/0003088-200847120-00003](https://doi.org/10.2165/0003088-200847120-00003) PMID: [19026034](https://pubmed.ncbi.nlm.nih.gov/19026034/)
8. Dupuis A, Tournier N, Le Moal G, Venisse N. Preparation and stability of voriconazole eye drop solution. *Antimicrob Agents Chemother*. 2009; 53:798–799. doi: [10.1128/AAC.01126-08](https://doi.org/10.1128/AAC.01126-08) PMID: [19001119](https://pubmed.ncbi.nlm.nih.gov/19001119/)
9. Amorós-Reboredo P, Bastida-Fernandez C, Guerrero-Molina L, Soy-Muner D, López-Cabezas C. Stability of frozen 1% voriconazole ophthalmic solution. *Am J Health Syst Pharm*. 2015; 72:479–482. doi: [10.2146/ajhp140127](https://doi.org/10.2146/ajhp140127) PMID: [25736943](https://pubmed.ncbi.nlm.nih.gov/25736943/)
10. Pahuja P, Kashyap H, Pawar P. Design and evaluation of HP- β -CD based voriconazole formulations for ocular drug delivery. *Curr Drug Deliv*. 2014; 11:223–232. PMID: [24365062](https://pubmed.ncbi.nlm.nih.gov/24365062/)
11. Pawar P, Kashyap H, Malhotra S, Sindhu R. Hp- β -CD-voriconazole in situ gelling system for ocular drug delivery: in vitro, stability, and antifungal activities assessment. *Biomed Res Int*. 2013; 2013:341218. doi: [10.1155/2013/341218](https://doi.org/10.1155/2013/341218) PMID: [23762839](https://pubmed.ncbi.nlm.nih.gov/23762839/)
12. Kumar R, Sinha VR. Preparation and optimization of voriconazole microemulsion for ocular delivery. *Colloids Surf B Biointerfaces*. 2014; 117:82–88. doi: [10.1016/j.colsurfb.2014.02.007](https://doi.org/10.1016/j.colsurfb.2014.02.007) PMID: [24632034](https://pubmed.ncbi.nlm.nih.gov/24632034/)
13. de Sá FA, Taveira SF, Gelfuso GM, Lima EM, Gratieri T. Liposomal voriconazole (VOR) formulation for improved ocular delivery. *Colloids Surf B Biointerfaces*. 2015; 133:331–338. doi: [10.1016/j.colsurfb.2015.06.036](https://doi.org/10.1016/j.colsurfb.2015.06.036) PMID: [26123854](https://pubmed.ncbi.nlm.nih.gov/26123854/)
14. Shukr MH. Novel in situ gelling ocular inserts for voriconazole-loaded niosomes: design, in vitro characterisation and in vivo evaluation of the ocular irritation and drug pharmacokinetics. *J Microencapsul*. 2016; 33:71–79. doi: [10.3109/02652048.2015.1128489](https://doi.org/10.3109/02652048.2015.1128489) PMID: [26739851](https://pubmed.ncbi.nlm.nih.gov/26739851/)
15. Goyal R, Macri LK, Kaplan HM, Kohn J. Nanoparticles and nanofibers for topical drug delivery. *J Control Release*. 2015 Oct 28. pii: S0168-3659 (15) 30215–7.
16. Jayaraman P, Gandhimathi C, Venugopal JR, Becker DL, Ramakrishna S, Srinivasan DK. Controlled release of drugs in electrosprayed nanoparticles for bone tissue engineering. *Adv Drug Deliv Rev*. 2015; 94:77–95. doi: [10.1016/j.addr.2015.09.007](https://doi.org/10.1016/j.addr.2015.09.007) PMID: [26415888](https://pubmed.ncbi.nlm.nih.gov/26415888/)
17. Sun XZ, Williams GR, Hou XX, Zhu LM. Electrospun curcumin-loaded fibers with potential biomedical applications. *Carbohydr Polym*. 2013; 94:147–153. doi: [10.1016/j.carbpol.2012.12.064](https://doi.org/10.1016/j.carbpol.2012.12.064) PMID: [23544523](https://pubmed.ncbi.nlm.nih.gov/23544523/)
18. Taepaiboon P, Rungsardthong U, Supaphol P, Taepaiboon P. Drug-loaded electrospun mats of poly (vinyl alcohol) fibres and their release characteristics of four model drugs. *Nanotechnology*. 2006; 17:2317–2329.
19. Sebe I, Szabó P, Kállai-Szabó B, Zekó R. Incorporating small molecules or biologics into nanofibers for optimized drug release: A review. *Int J Pharm*. 2015; 494:516–530. doi: [10.1016/j.ijpharm.2015.08.054](https://doi.org/10.1016/j.ijpharm.2015.08.054) PMID: [26307263](https://pubmed.ncbi.nlm.nih.gov/26307263/)

20. Hermans K, Van den Plas D, Kerimova S, Carleer R, Adriaenssens P, Weyenberg W, et al. Development and characterization of mucoadhesive chitosan films for ophthalmic delivery of cyclosporine A. *Int J Pharm.* 2014; 472:10–19. doi: [10.1016/j.ijpharm.2014.06.017](https://doi.org/10.1016/j.ijpharm.2014.06.017) PMID: [24929014](https://pubmed.ncbi.nlm.nih.gov/24929014/)
21. Sifaka PI, Üstündağ Okur N, Mone M, Giannakopoulou S, Er S, Pavlidou E, et al. Two different approaches for oral administration of voriconazole loaded formulations: electrospun fibers versus β -cyclodextrin complexes. *Int J Mol Sci.* 2016; 17:E282. doi: [10.3390/ijms17030282](https://doi.org/10.3390/ijms17030282) PMID: [26927072](https://pubmed.ncbi.nlm.nih.gov/26927072/)
22. Shukr M. Formulation, in vitro and in vivo evaluation of lidocaine HCl ocular inserts for topical ocular anesthesia. *Arch Pharm Res.* 2014; 37:882–889. doi: [10.1007/s12272-013-0317-x](https://doi.org/10.1007/s12272-013-0317-x) PMID: [24395530](https://pubmed.ncbi.nlm.nih.gov/24395530/)
23. Jain D, Carvalho E, Banthia AK, Banerjee R. Development of polyvinyl alcohol-gelatin membranes for antibiotic delivery in the eye. *Drug Dev Ind Pharm.* 2011; 37:167–177. doi: [10.3109/03639045.2010.502533](https://doi.org/10.3109/03639045.2010.502533) PMID: [21073319](https://pubmed.ncbi.nlm.nih.gov/21073319/)
24. Xu J, Li X, Sun F, Cao P. PVA hydrogels containing beta-cyclodextrin for enhanced loading and sustained release of ocular therapeutics. *J Biomater Sci Polym Ed.* 2010; 21:1023–1038. doi: [10.1163/156856209X463690](https://doi.org/10.1163/156856209X463690) PMID: [20507706](https://pubmed.ncbi.nlm.nih.gov/20507706/)
25. Higuchi T, Connors KA. Phase-solubility techniques. In: *Relley CN, editors. Advances in analytical chemistry and instrumentation.* New York: Wiley-Interscience; 1965. pp.117–212.
26. Karn PR, Kim HD, Kang H, Sun BK, Jin SE, Hwang SJ. Supercritical fluid-mediated liposomes containing cyclosporin A for the treatment of dry eye syndrome in a rabbit model: comparative study with the conventional cyclosporin emulsion. *Int J Nanomedicine.* 2014; 9:3791–3800. doi: [10.2147/IJN.S65601](https://doi.org/10.2147/IJN.S65601) PMID: [25143728](https://pubmed.ncbi.nlm.nih.gov/25143728/)
27. Szente L, Szejtli J. Highly soluble cyclodextrin derivatives: chemistry, properties, and trends in development. *Adv Drug Deliv Rev.* 1999; 36:17–28. PMID: [10837706](https://pubmed.ncbi.nlm.nih.gov/10837706/)
28. Pahuja P, Kashyap H, Pawar P. Design and evaluation of HP- β -CD based voriconazole formulations for ocular drug delivery. *Curr Drug Deliv.* 2014; 11:223–232. PMID: [24365062](https://pubmed.ncbi.nlm.nih.gov/24365062/)
29. Delvalle E. Cyclodextrins and their uses: a review. *Process Biochemistry.* 2004; 39: 1033–1046.
30. Luke DR, Tomaszewski K, Damle B, Schlamm HT. Review of the basic and clinical pharmacology of sulfobutylether-beta-cyclodextrin (SBECD). *J Pharm Sci.* 2010; 99:3291–3301. doi: [10.1002/jps.22109](https://doi.org/10.1002/jps.22109) PMID: [20213839](https://pubmed.ncbi.nlm.nih.gov/20213839/)
31. Tonglairoom P, Ngawhirunpat T, Rojanarata T, Kaomongkolgit R, Opanasopit. Fabrication and evaluation of nanostructured herbal oil/hydroxypropyl- β -cyclodextrin/polyvinylpyrrolidone mats for denture stomatitis prevention and treatment. *AAPS Pharm Sci Tech.* 2016;
32. DiLuccio RC, Hussain MA, Coffin-Beach D, Torosian G, Shefter E, Hurwitz AR. Sustained-release oral delivery of theophylline by use of polyvinyl alcohol and polyvinyl alcohol-methyl acrylate polymers. *J Pharm Sci.* 1994; 83:104–106. PMID: [8138896](https://pubmed.ncbi.nlm.nih.gov/8138896/)
33. Schulze J, Hendriks S, Schulz-Siegmund M, Aigner A. Microparticulate poly (vinyl alcohol) hydrogel formulations for embedding and controlled release of polyethylenimine (PEI)-based nanoparticles. *Acta Biomater.* 2016 Sep 2. pii: S1742-7061(16)30461-5.
34. Negishi J, Nam K, Kimura T, Fujisato T, Kishida A. High-hydrostatic pressure technique is an effective method for the preparation of PVA-heparin hybrid gel. *Eur J Pharm Sci.* 2010; 41:617–622. doi: [10.1016/j.ejps.2010.09.001](https://doi.org/10.1016/j.ejps.2010.09.001) PMID: [20833248](https://pubmed.ncbi.nlm.nih.gov/20833248/)
35. Nafee NA, Ismail FA, Boraie NA, Mortada LM. Mucoadhesive buccal patches of miconazole nitrate: in vitro/in vivo performance and effect of ageing. *Int J Pharm.* 2003; 264:1–14. PMID: [12972331](https://pubmed.ncbi.nlm.nih.gov/12972331/)
36. Reynolds TD, Mitchell SA, Balwinski KM. Investigation of the effect of tablet surface area/volume on drug release from hydroxypropylmethylcellulose controlled-release matrix tablets. *Drug Dev Ind Pharm.* 2002; 28:457–466. doi: [10.1081/DDC-120003007](https://doi.org/10.1081/DDC-120003007) PMID: [12056539](https://pubmed.ncbi.nlm.nih.gov/12056539/)
37. Saettone MF <http://www.sciencedirect.com/science/article/pii/0169409X9500014X>—COR1, Salminen L. Ocular inserts for topical delivery. *Adv Drug Deliv. Rev.* 1995; 16:95–106.
38. Tonglairoom P, Ngawhirunpat T, Rojanarata T, Kaomongkolgit R, Opanasopit P. Fast-acting clotrimazole composited PVP/HP β CD nanofibers for oral candidiasis application. *Pharm Res.* 2014; 31:1893–1906. doi: [10.1007/s11095-013-1291-1](https://doi.org/10.1007/s11095-013-1291-1) PMID: [24554117](https://pubmed.ncbi.nlm.nih.gov/24554117/)
39. Miletic T, Kyriakos K, Graovac A, Ibric S. Spray-dried voriconazole-cyclodextrin complexes: solubility, dissolution rate and chemical stability. *Carbohydr Polym.* 2013; 98:122–131. doi: [10.1016/j.carbpol.2013.05.084](https://doi.org/10.1016/j.carbpol.2013.05.084) PMID: [23987325](https://pubmed.ncbi.nlm.nih.gov/23987325/)
40. Yang W, Chow KT, Lang B, Wiederhold NP, Johnston KP, Williams RO. In vitro characterization and pharmacokinetics in mice following pulmonary delivery of itraconazole as cyclodextrin solubilized solution. *Eur J Pharm Sci.* 2010; 39:336–347. doi: [10.1016/j.ejps.2010.01.001](https://doi.org/10.1016/j.ejps.2010.01.001) PMID: [20093186](https://pubmed.ncbi.nlm.nih.gov/20093186/)
41. Peeters J, Neeskens P, Tollenaere JP, Van Remoortere P, Brewster ME. Characterization of the interaction of 2-hydroxypropyl- β -cyclodextrin with itraconazole at pH 2, 4, and 7. *J Pharm Sci.* 2002; 91:1414–1422. doi: [10.1002/jps.10126](https://doi.org/10.1002/jps.10126) PMID: [12115841](https://pubmed.ncbi.nlm.nih.gov/12115841/)

42. Duxfield L, Sultana R, Wang R, Englebretsen V, Deo S, Rupenthal ID, et al. Ocular delivery systems for topical application of anti-infective agents. *Drug Dev Ind Pharm*. 2015 Sep 1.
43. Morrison PW, Connon CJ, Khutoryanskiy VV. Cyclodextrin-mediated enhancement of riboflavin solubility and corneal permeability. *Mol Pharm*. 2013; 10:756–762. doi: [10.1021/mp3005963](https://doi.org/10.1021/mp3005963) PMID: [23294178](https://pubmed.ncbi.nlm.nih.gov/23294178/)
44. Li GX, Gu X, Song HY, Nan KH, Chen H. Biocompatibility and drug release behavior of chitosan/poly (vinyl alcohol) corneal shield in vivo. *Int J Clin Exp Med*. 2015; 8:12949–12955. PMID: [26550213](https://pubmed.ncbi.nlm.nih.gov/26550213/)
45. Loftssona T, Järvinen T. Cyclodextrins in ophthalmic drug delivery. *Adv Drug Deliv Rev*. 1996; 36:59–79.